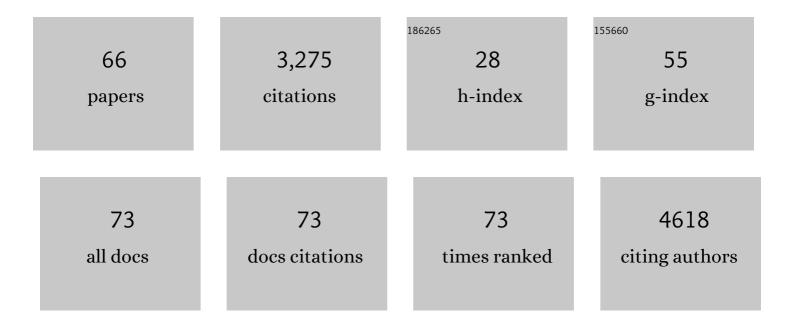
List of Publications by Year in descending order

Source: https://exaly.com/author-pdf/2224902/publications.pdf Version: 2024-02-01



MADE D FOSTED

#	Article	IF	CITATIONS
1	Nearest-Neighbor Effects Modulate <i>loxP</i> Spacer DNA Chemical Shifts and Guide Oligonucleotide Design for Nuclear Magnetic Resonance Studies. Biochemistry, 2022, 61, 67-76.	2.5	0
2	Mechanisms of Cre recombinase synaptic complex assembly and activation illuminated by Cryo-EM. Nucleic Acids Research, 2022, 50, 1753-1769.	14.5	6
3	Elucidation of structure–function relationships in <i>Methanocaldococcus jannaschii</i> RNase P, a multi-subunit catalytic ribonucleoprotein. Nucleic Acids Research, 2022, 50, 8154-8167.	14.5	5
4	Epidemiological and cohort study finds no association between COVID-19 and Guillain-Barré syndrome. Brain, 2021, 144, 682-693.	7.6	221
5	Rational design of cell-permeable cyclic peptides containing a d-Pro-l-Pro motif. Bioorganic and Medicinal Chemistry, 2020, 28, 115711.	3.0	10
6	DNA binding induces a <i>cis</i> -to- <i>trans</i> switch in Cre recombinase to enable intasome assembly. Proceedings of the National Academy of Sciences of the United States of America, 2020, 117, 24849-24858.	7.1	4
7	Population Distributions from Native Mass Spectrometry Titrations Reveal Nearest-Neighbor Cooperativity in the Ring-Shaped Oligomeric Protein TRAP. Biochemistry, 2020, 59, 2518-2527.	2.5	8
8	The Loz1 transcription factor from <i>Schizosaccharomyces pombe</i> binds to Loz1 response elements and represses gene expression when zinc is in excess. Molecular Microbiology, 2019, 112, 1701-1717.	2.5	3
9	MicroRNAs as Novel Biomarkers for the Diagnosis and Prognosis of Mild and Severe Traumatic Brain Injury. Journal of Neurotrauma, 2017, 34, 1948-1956.	3.4	147
10	Mechanistic Models Fit to Variable Temperature Calorimetric Data Provide Insights into Cooperativity. Biophysical Journal, 2017, 112, 1328-1338.	0.5	5
11	Conformational and chemical selection by a <i>trans</i> -acting editing domain. Proceedings of the National Academy of Sciences of the United States of America, 2017, 114, E6774-E6783.	7.1	19
12	Structure of the Brd4 ET domain bound to a C-terminal motif from Î <sup>3</sup> -retroviral integrases reveals a conserved mechanism of interaction. Proceedings of the National Academy of Sciences of the United States of America, 2016, 113, 2086-2091.	7.1	65
13	pH Dependence of the Stress Regulator DksA. PLoS ONE, 2015, 10, e0120746.	2.5	22
14	MESMER: minimal ensemble solutions to multiple experimental restraints. Bioinformatics, 2015, 31, 1951-1958.	4.1	10
15	Bimodal high-affinity association of Brd4 with murine leukemia virus integrase and mononucleosomes. Nucleic Acids Research, 2014, 42, 4868-4881.	14.5	37
16	The L7Ae protein binds to two kink-turns in the Pyrococcus furiosus RNase P RNA. Nucleic Acids Research, 2014, 42, 13328-13338.	14.5	15
17	Gene regulation by substoichiometric heterocomplex formation of undecameric TRAP and trimeric anti-TRAP. Proceedings of the National Academy of Sciences of the United States of America, 2014, 111, 3442-3447.	7.1	13
18	Uncovering the Stoichiometry of <i>Pyrococcus furiosus</i> RNase P, a Multiâ€5ubunit Catalytic Ribonucleoprotein Complex, by Surfaceâ€Induced Dissociation and Ion Mobility Mass Spectrometry. Angewandte Chemie - International Edition, 2014, 53, 11483-11487.	13.8	32

#	Article	IF	CITATIONS
19	DksA2, a zincâ€ <del>i</del> ndependent structural analog of the transcription factor DksA. FEBS Letters, 2013, 587, 614-619.	2.8	33
20	Homotropic Cooperativity from the Activation Pathway of the Allosteric Ligand-Responsive Regulatory <i>trp</i> RNA-Binding Attenuation Protein. Biochemistry, 2013, 52, 8855-8865.	2.5	4
21	Structural basis for high-affinity binding of LEDGF PWWP to mononucleosomes. Nucleic Acids Research, 2013, 41, 3924-3936.	14.5	182
22	Interaction of the HIV-1 Intasome with Transportin 3 Protein (TNPO3 or TRN-SR2). Journal of Biological Chemistry, 2012, 287, 34044-34058.	3.4	52
23	Fidelity of tRNA 5â€2-maturation: a possible basis for the functional dependence of archaeal and eukaryal RNase P on multiple protein cofactors. Nucleic Acids Research, 2012, 40, 4666-4680.	14.5	14
24	Thermodynamics of Coupled Folding in the Interaction of Archaeal RNase P Proteins RPP21 and RPP29. Biochemistry, 2012, 51, 926-935.	2.5	13
25	Mechanisms of Allosteric Gene Regulation by NMR Quantification of Microsecond–Millisecond Protein Dynamics. Journal of Molecular Biology, 2012, 415, 372-381.	4.2	17
26	GUARDD: user-friendly MATLAB software for rigorous analysis of CPMG RD NMR data. Journal of Biomolecular NMR, 2012, 52, 11-22.	2.8	40
27	Tuning Riboswitch Regulation through Conformational Selection. Journal of Molecular Biology, 2011, 405, 926-938.	4.2	48
28	Cooperative RNP Assembly: Complementary Rescue of Structural Defects by Protein and RNA Subunits of Archaeal RNase P. Journal of Molecular Biology, 2011, 411, 368-383.	4.2	11
29	Assembly of the Complex between Archaeal RNase P Proteins RPP30 and Pop5. Archaea, 2011, 2011, 1-12.	2.3	8
30	An introduction to NMR-based approaches for measuring protein dynamics. Biochimica Et Biophysica Acta - Proteins and Proteomics, 2011, 1814, 942-968.	2.3	419
31	Response rates in GP surveys - trialling two recruitment strategies. Australian Family Physician, 2011, 40, 427-30.	0.5	93
32	Mechanism for pH-dependent gene regulation by amino-terminus-mediated homooligomerization of <i>Bacillus subtilis</i> anti- <i>trp</i> RNA-binding attenuation protein. Proceedings of the National Academy of Sciences of the United States of America, 2010, 107, 15385-15390.	7.1	5
33	Mapping the surface of Escherichia coli peptide deformylase by NMR with organic solvents. Protein Science, 2009, 11, 1850-1853.	7.6	18
34	Ligand-Induced Changes in the Structure and Dynamics of Escherichia coli Peptide Deformylase. Biochemistry, 2009, 48, 7595-7607.	2.5	10
35	Solution Structure of an Archaeal RNase P Binary Protein Complex: Formation of the 30-kDa Complex between Pyrococcus furiosus RPP21 and RPP29 Is Accompanied by Coupled Protein Folding and Highlights Critical Features for Protein–Protein and Protein–RNA Interactions. Journal of Molecular Biology, 2009, 393, 1043-1055.	4.2	37
36	Crystallization and structure determination of the core-binding domain of bacteriophage lambda integrase. Acta Crystallographica Section F: Structural Biology Communications, 2008, 64, 470-473.	0.7	4

#	Article	IF	CITATIONS
37	Solution Structure of <i>Pyrococcus furiosus</i> RPP21, a Component of the Archaeal RNase P Holoenzyme, and Interactions with Its RPP29 Protein Partner. Biochemistry, 2008, 47, 11704-11710.	2.5	27
38	Identification of the oril-Binding Site of Poliovirus 3C Protein by Nuclear Magnetic Resonance Spectroscopy. Journal of Virology, 2008, 82, 4363-4370.	3.4	16
39	Mandatory protocol for treating adult patients with diabetic ketoacidosis decreases intensive care unit and hospital lengths of stay: Results of a nonrandomized trial*. Critical Care Medicine, 2007, 35, 41-46.	0.9	152
40	Trans Cooperativity by a Split DNA Recombinase: The Central and Catalytic Domains of Bacteriophage Lambda Integrase Cooperate in Cleaving DNA Substrates When the Two Domains Are not Covalently Linked. Journal of Molecular Biology, 2007, 370, 303-314.	4.2	2
41	DNA Recognition via Mutual-Induced Fit by the Core-Binding Domain of Bacteriophage λ Integrase. Biochemistry, 2007, 46, 13939-13947.	2.5	5
42	Solution NMR of Large Molecules and Assembliesâ€. Biochemistry, 2007, 46, 331-340.	2.5	141
43	Thermodynamics of Tryptophan-Mediated Activation of thetrpRNA-Binding Attenuation Proteinâ€. Biochemistry, 2006, 45, 7844-7853.	2.5	23
44	Structure of Pfu Pop5, an archaeal RNase P protein. Proceedings of the National Academy of Sciences of the United States of America, 2006, 103, 873-878.	7.1	55
45	Protein folding coupled to DNA binding in the catalytic domain of bacteriophage lambda integrase detected by mass spectrometry. Protein Science, 2003, 12, 620-626.	7.6	19
46	Mechanism of Flavin Mononucleotide Cofactor Binding to the Desulfovibrio vulgaris Flavodoxin. 2. Evidence for Cooperative Conformational Changes Involving Tryptophan 60 in the Interaction between the Phosphate- and Ring-Binding Subsites. Biochemistry, 2003, 42, 2317-2327.	2.5	16
47	Dynamics and DNA Substrate Recognition by the Catalytic Domain of Lambda Integrase. Journal of Molecular Biology, 2003, 329, 423-439.	4.2	19
48	Preparation of uniformly labeled NMR samples in Escherichia coli under the tight control of the araBAD promoter: expression of an archaeal homolog of the RNase P Rpp29 protein. Protein Expression and Purification, 2003, 28, 246-251.	1.3	8
49	Structure of Mth11/Mth Rpp29, an essential protein subunit of archaeal and eukaryotic RNase P. Proceedings of the National Academy of Sciences of the United States of America, 2003, 100, 15398-15403.	7.1	47
50	TROSY-NMR Studies of the 91kDa TRAP Protein Reveal Allosteric Control of a Gene Regulatory Protein by Ligand-altered Flexibility. Journal of Molecular Biology, 2002, 323, 463-473.	4.2	78
51	Characterization of Ad5 E3-14.7K, an adenoviral inhibitor of apoptosis: Structure, oligomeric state, and metal binding. Protein Science, 2002, 11, 1117-1128.	7.6	11
52	Chemical shift as a probe of molecular interfaces: NMR studies of DNA binding by the three amino-terminal zinc finger domains from transcription factor IIIA. Journal of Biomolecular NMR, 1998, 12, 51-71.	2.8	110
53	Three-Dimensional Solution Structure of Conotoxin Ï^Piiie, an Acetylcholine Gated Ion Channel Antagonistâ€,‡. Biochemistry, 1998, 37, 1215-1220.	2.5	21
54	High-resolution solution structure of the retinoid X receptor DNA-binding domain. Journal of Molecular Biology, 1998, 281, 271-284.	4.2	58

#	Article	IF	CITATIONS
55	Solution structure of the first three zinc fingers of TFIIIA bound to the cognate DNA sequence: determinants of affinity and sequence specificity. Journal of Molecular Biology, 1997, 273, 183-206.	4.2	182
56	Domain packing and dynamics in the DNA complex of the N-terminal zinc fingers of TFIIIA. Nature Structural Biology, 1997, 4, 605-608.	9.7	116
57	Interaction of the RNA binding Fingers ofXenopusTranscription Factor IIIA with Specific Regions of 5 S Ribosomal RNA. Journal of Molecular Biology, 1995, 248, 44-57.	4.2	47
58	Bistramides A, B, C, D, and K: A New Class of Bioactive Cyclic Polyethers from Lissoclinum bistratum. Journal of Natural Products, 1994, 57, 1336-1345.	3.0	70
59	Nairaiamides A and B. two novel di-proline heptapeptides isolated from a fijian Lissoclinum bistratum ascidian Tetrahedron Letters, 1993, 34, 2871-2874.	1.4	16
60	Biomedical Potential of Marine Natural Products. , 1993, , 1-43.		60
61	Bistratamides C and D. Two new oxazole-containing cyclic hexapeptides isolated from a Philippine Lissoclinum bistratum ascidian. Journal of Organic Chemistry, 1992, 57, 6671-6675.	3.2	102
62	Tawicyclamides A and B, new cyclic peptides from the Ascidian Lissoclinum patella: studies on the solution- and solid-state conformations. Journal of Organic Chemistry, 1992, 57, 4616-4624.	3.2	69
63	Revised structure of bistramide A (bistratene A): application of a new program for the automated analysis of 2D INADEQUATE spectra. Journal of the American Chemical Society, 1992, 114, 1110-1111.	13.7	67
64	Applications of the improved computerized analysis of 2D INADEQUATE spectra. Analytical Chemistry, 1992, 64, 3150-3160.	6.5	31
65	Studies on the solution- and solid-state structure of patellin 2. Journal of the American Chemical Society, 1990, 112, 8080-8084.	13.7	52
66	Natural Product Peptides from Marine Organisms. Bioorganic Marine Chemistry, 1989, , 1-46.	0.2	23